

# RSC Advances



This is an *Accepted Manuscript*, which has been through the Royal Society of Chemistry peer review process and has been accepted for publication.

*Accepted Manuscripts* are published online shortly after acceptance, before technical editing, formatting and proof reading. Using this free service, authors can make their results available to the community, in citable form, before we publish the edited article. This *Accepted Manuscript* will be replaced by the edited, formatted and paginated article as soon as this is available.

You can find more information about *Accepted Manuscripts* in the [Information for Authors](#).

Please note that technical editing may introduce minor changes to the text and/or graphics, which may alter content. The journal's standard [Terms & Conditions](#) and the [Ethical guidelines](#) still apply. In no event shall the Royal Society of Chemistry be held responsible for any errors or omissions in this *Accepted Manuscript* or any consequences arising from the use of any information it contains.

**Bio-based Polyurethanes with Shape Memory Behavior at Body  
Temperature: Effect of Different Chain Extenders**

Lin Gu<sup>1\*</sup>, Bin Cui<sup>1,3</sup>, Qing-Yun Wu<sup>2</sup>, Haibin Yu<sup>1\*</sup>

<sup>1</sup>Key Laboratory of Marine Materials and Related Technologies, Key Laboratory of Marine Materials and Protective Technologies of Zhejiang Province, Ningbo Institute of Materials Technology and Engineering, Chinese Academy of Sciences, Ningbo 315201, P. R. China

<sup>2</sup>Department of Polymer Science and Engineering, Faculty of Materials Science and Chemical Engineering, Ningbo University, Ningbo 315211, P. R. China

<sup>3</sup>Department of Polymer and Coating, Jiangxi Science & Technology Normal University, Nanchang 330013, China

---

\* Corresponding author: Tel.: +86 0574 87911126.

E-mail addresses: gulin1985@gmail.com; haibinyu@nimte.ac.cn

### Abstract

In this work, a series of bio-based shape memory polyurethanes were synthesized from polylactide copolymer diols, isophorone diisocyanate (IPDI) and chain extenders, in which the chain extenders are used to adjust their transition temperatures and shape memory properties. These bio-based polyurethanes (bio-PU) show a  $T_g$  in the range of 28.7-34 °C, which is very closed to the body temperature and can be adjusted by the carbon chain length of the chain extenders. Moreover, they have low Young's modulus (34.7 MPa) and high elongation (434.0%). Through a serial of shape memory tests, the bio-PU exhibit good shape memory behavior at the body temperature with a shape recovery rate greater than 90%. Especially, the bio-PU from 1,4-cyclohexanedimethanol (CHDM) with non-planar ring structure displays the highest shape recovery rate, which may be due to that CHDM in the hard segments acts as “molecular spring”. Therefore, these shape memory bio-PU are expected to have many practical applications in medical devices.

**Keywords:** polylactide polyol, shape memory polyurethane, biodegradable, bio-based, chain extender

## 1. Introduction

Shape memory polymers (SMPs) are considered as smart materials that are able to change their shapes for responding to external stimulus, such as temperature, light, electricity, pH and so on.<sup>1-4</sup> SMPs have been widely applied in biomedical devices, including cardiovascular stents,<sup>5</sup> sutures,<sup>6</sup> drug-eluting stents,<sup>7</sup> clot removal devices,<sup>8</sup> tissue engineering,<sup>10</sup> etc., where SMPs are often required biocompatibility, biodegradability, and a shape recovery temperature close to human body temperature.<sup>11</sup> Among them, shape memory polyurethanes (SMPUs) are known to be promisingly responsive materials when used as biomedical devices in the body because of their adjustable transition temperatures for shape recovery and good biocompatibility.<sup>12-17</sup> Hasan et al. developed SMPU foam embolic devices with slower actuation times by incorporating isophorone diisocyanate (IPDI) into the foam matrix.<sup>18</sup> IPDI in the foam played a key role in elongating the working time and delaying water plasticization of the material. Singhal et al. synthesized a series of novel biodegradable SMPU foams for embolic biomedical applications by use of the degradable polycaprolactone triol (PCL-t).<sup>19</sup> The degradation rate of the materials could be controlled by changing the PCL-t content and the material hydrophobicity.

On the other hand, SMPUs from biomass sources have drawn a great deal of attention due to environmental concerns and the rapid consumption of petroleum.<sup>20-22</sup> The most popular bio-based SMPUs (bio-SMPUs) are currently derived from vegetable oils.<sup>23-25</sup> However, one obvious shortcoming of vegetable oils-based SMPUs is their poor mechanical properties (e.g. low elongation at break) compared to

those petroleum-based SMPUs.<sup>26, 27</sup> This is because the long dangling chains in the vegetable oil polyols have an adverse effect on the micro-phase separation of the polyurethanes (PUs). Zhu et al. reported that bio-SMPUs with short side chains were prepared from bio-based polyester diols.<sup>17</sup> The short branch chains barely have effect on the phase separation, and consequently their mechanical properties are satisfactory. Zhu et al. also developed a bio-SMPU by substituting a petroleum based chain extender with a rosin based one.<sup>21</sup> With the careful molecular design, they constructed highly incompatible hard and soft segments along the polymer chains, and the obtained SMPUs with supreme shape recovery property. However, the shape recovery temperature of rosin-based SMPUs is much below the body temperature, which are not particularly suitable for biomedical uses. Recently, a series of SMPs based on bio-based polylactide (PLA) have been reported due to their good biocompatibility and biodegradability.<sup>28-33</sup> For example, Jing et al. reported PLA-based SMPs with glass transition temperature ( $T_g$ ) in the range of 33-63 °C were prepared from PLA diols, diisocyanate compounds and 1,4-butanediol (BDO).<sup>32, 33</sup> The  $T_g$  could be adjusted by the molecular weight of PLA diols. However, the PLA-based SMPUs exhibit relatively low elongation at break and high Young's modulus.

In this work, a series of bio-based polyurethanes (bio-PUs) with shape memory behaviors at body temperature were prepared, in which the chain extenders are used to adjust their transition temperatures and shape memory properties. The obtained bio-PUs have high elongation (434.0%) and low Young's modulus (34.7 MPa). Through a series of shape memory tests, the bio-SMPUs exhibit good shape memory

behaviors at body temperature with a shape recovery rate greater than 90%. These bio-SMPUs are expected to have many practical applications in medical devices.

## 2. Experimental section

### 2.1 Materials

Stannous octoate ( $\text{SnOct}_2$ ), isophorone diisocyanate (IPDI), 1,4-butanediol (BDO), 1,6-hexanediol (HDO) and 1,4-cyclohexanedimethanol (CHDM) were purchased from Aladdin Industrial Corporation (Shanghai, China). Ethylene glycol (EG), tetrahydrofuran (THF), *N,N*-dimethyl formamide (DMF), di-*n*-butylamine and hydrochloric acid (HCl) are analytically pure, and were obtained from Sinopharm Chemical Reagent Co., Ltd (Shanghai, China). 1, 12-Dodecanediol (DDO) was purchased from TCI (Shanghai, China) and used as received. *L*-lactide (LA) and  $\epsilon$ -caprolactone (CL) were provided from Shenzhen Esun Industrial Co., Ltd (Shenzhen, China).

### 2.2 Synthesis of polylactide copolymer diols and Preparation of bio-PU

The series of poly(lactide-co-caprolactone) diols (co-PLAols) were synthesized by ring opening polymerization of LA and CL using  $\text{SnOct}_2$  as a catalyst and BDO as a chain transferring agent. In a  $\text{N}_2$  atmosphere, LA, CL, BDO and  $\text{SnOct}_2$  were added to 2-L flask free of oxygen and water, where the feed molar ratio of LA and CL was 3.17 and the amount of  $\text{SnOct}_2$  was 0.1% with respect to monomers (LA and CL), wt/wt. The reaction was carried out at 160 °C for 6 h. The molecular weight of co-PLAol was adjusted to be 1000, 2000 and 3000 g/mol by changing the feed molar ratio of BDO and monomers (1/6.6, 1/13.3, 1/21.3), which were denoted as

co-PLAol-1000, co-PLAol-2000 and co-PLAol-3000, respectively.

The bio-PUs were prepared by a two-step polymerization process, as shown in Scheme 1. The molar ratio of co-PLAol-3000, IPDI and the chain extender was 1:2:1. The obtained bio-based polyurethane was nominated as bio-PU-xxx, in which xxx indicates the chain extender. The detail information of the obtained bio-PUs is summarized in Table 1.

### 2.3 Characterization

FTIR spectra were obtained on a Thermo Nicolet 6700 spectrometer using the attenuated total reflection (ATR) mode.  $^1\text{H}$  NMR spectra were recorded on a Bruker AV-400 NMR spectrometer in deuterated chloroform. The number and weight average molecular weights ( $M_n$ ,  $M_w$ ) of bio-PUs were measured on a HLC-8320 gel permeation chromatography (GPC) according to polystyrene standard using THF as eluent.

Differential scanning calorimetry (DSC) analysis was performed on a DSC 214 Polyma instrument under a  $\text{N}_2$  atmosphere. The samples were initially heated from  $-30\text{ }^\circ\text{C}$  to  $180\text{ }^\circ\text{C}$ , then cooled to  $-30\text{ }^\circ\text{C}$ , and followed by heating to  $180\text{ }^\circ\text{C}$  at a rate of  $10\text{ }^\circ\text{C}/\text{min}$ . The glass transition temperature ( $T_g$ ) was determined from the second heating curve to eliminate the thermal history. Thermo gravimetric analysis (TGA) was carried out on a PerkinElmer Pyris Diamond thermal analyzer at a heating rate of  $20\text{ }^\circ\text{C}/\text{min}$  from  $40\text{ }^\circ\text{C}$  to  $500\text{ }^\circ\text{C}$  under a  $\text{N}_2$  atmosphere. Tapping mode atomic force microscopy (AFM) was conducted on a scanning probe microscope (Dimension 3100 V). The AFM sample was prepared by casting the bio-PU solution (5 wt%) on a

silicon wafer. The samples were measured at least twice by DSC, TGA, and AFM.

Tensile tests were performed on an Instron 5567 instrument with a speed of 100 mm/min at 25 °C according to ASTM standard (ASTM D638). The data reported were the mean value of five determinations. Cyclic tensile tests were also performed on the same machine according the reference.<sup>17</sup> First, the dumbbell-shaped sample of 2 mm width, 35 mm length, and 1 mm thickness was stretched to  $\varepsilon_m$ , 200% elongation at 25 °C with a speed of 100 mm/min. Then, the clamps began to return at a speed of 20 mm/min until the force on the sample was 0. After the above two steps, one cycle is complete. Every sample was subjected to 5 cycles and the shape recovery rate ( $R_r$ ) was calculated by the following formula.

$$R_r(N) = \frac{\varepsilon_m - \varepsilon_p(N)}{\varepsilon_m - \varepsilon_p(N-1)} \times 100\%$$

where  $N$  is the cycle number,  $\varepsilon_m$  is the maximum strain imposed on the material,  $\varepsilon_p(N)$  and  $\varepsilon_p(N-1)$  are the strains of the sample in two successive cycles when the force on the sample is 0, and  $R_r(N)$  is based on two successive cycles.

The program of the shape memory test of bio-PU was conducted as follows: Firstly, the specimens were bent to a given angle at 37 °C. Subsequently, they were quenched below  $T_g$  using liquid nitrogen. Then the samples were allowed for free recovery at 37 °C.

### 3. Results and discussion

#### 3.1 Synthesis and characterization of bio-PU

In order to get the bio-SMPUs with large elongation at break and low Young's modulus, co-PLAols were used as the soft segment to substitute for PLA diols. As



shown in Scheme 1, the bio-PU were prepared via a two-step polymerization process, which were characterized by FTIR and  $^1\text{H}$  NMR spectra. Figure 1 shows the FTIR spectra of the obtained bio-PU. These FTIR spectra are very similar, and they exhibit NH absorption peaks at ca.  $3360\text{ cm}^{-1}$  and amide II absorption bands at ca.  $1530\text{ cm}^{-1}$  characteristic of urethane groups, while the  $\text{N}=\text{C}=\text{O}$  stretching vibration bands at  $2270\text{ cm}^{-1}$  and OH stretching peaks at ca.  $3500\text{ cm}^{-1}$  are characteristic of co-PLAol disappear. This result indicates that all IPDI has reacted with co-PLAol and the chain extender. Moreover, the absorption peaks at ca.  $1750$  and  $1200\text{ cm}^{-1}$  are attributed to the stretching vibrations of  $\text{C}=\text{O}$  and  $\text{C}-\text{O}-\text{C}$  in the ester units of co-PLAol, respectively.

The  $^1\text{H}$  NMR spectra of the obtained bio-PU are as shown as Figure 2. In all spectra, the signals at 5.17 ppm are assigned to the  $-\text{CH}-$  connected to  $\text{C}=\text{O}$  in co-PLAol, and the signals at 2.32, 1.64, 1.29, 1.62, 4.08 ppm are ascribed to protons on  $-\text{C}=\text{O}-\text{CH}_2-\text{CH}_2-\text{CH}_2-\text{CH}_2-\text{CH}_2-\text{O}-$  in co-PLAol, respectively. Additionally, peaks at 2.88 ppm are attributed to  $-\text{CH}_2-$  between  $\text{NH}-\text{COO}-$  and hexatomic ring, and the protons on hexatomic ring connected to  $\text{NH}-\text{COO}-$  appear at 3.74 ppm, indicating the reactions of IPDI with co-PLAol and the chain extender. Furthermore, the protons on the chain extenders have also been assigned in Figure 2.

The above results demonstrate that the bio-PU with different chain extenders were successfully prepared. The thermal, mechanical and shape memory properties of the obtained bio-PU would be discussed in the following sections.

### 3.2 Thermal and Mechanical Properties of bio-PU

Figure 3 displays the DSC curves of the obtained bio-PU with different chain extenders, and their  $T_g$  values are listed in Table 2. All synthesized bio-PU show only one  $T_g$  but no melting or crystallization peaks in the DSC curves, suggesting that the synthesized bio-PU were amorphous.<sup>20</sup> As the carbon chain length of the chain extender increases from bio-PU-EG to bio-PU-DDO, the  $T_g$  values decrease from 34.0 °C to 28.7 °C, possibly due to the increase of the chain flexibility. The  $T_g$  value of bio-PU-CHDM is 34 °C as same as bio-PU-EG. For amorphous PUs,  $T_g$  serves as the shape transition temperature ( $T_{trans}$ ).<sup>34, 35</sup> Hence, it is clear that the  $T_{trans}$  values of all synthesized bio-PU are very closed to body temperature. These synthesized bio-PU are expected to have many applications in medical devices.

The thermal stability of bio-PU was investigated by TGA. Figure 4 shows the TGA weight loss curves of the obtained bio-PU, and their weight loss temperatures are summarized in Table 2. From Table 2, the  $T_{5\%}$  and  $T_{max}$  of all synthesized bio-PU are above 200 and 300 °C, respectively, suggesting a good thermal stability of these PUs. Moreover, the bio-PU-CHDM exhibits better thermal stability than other bio-PU, because of the richer cyclic component in its main chain.<sup>36</sup>

Figure 5 shows the typical stress-strain curves of the synthesized bio-PU from different chain extenders. A yielding could be obviously observed before break. Table 2 summarizes specific tensile strength, elongation and Young's modulus of each PU. From Table 2, all the bio-PU have low Young's modulus (34.7 MPa) and high elongation (434.0%). The tensile strength of these PUs is 2.3-3.2 MPa. Except for bio-PU-EG, the elongations of all bio-PU range from 372.6% to 434.0%. As the

carbon chain length of the chain extender increases from bio-PU-EG to bio-PU-BDO, the elongation increases from 261.3% to 434%, which is ascribed to the short carbon chain of EG, resulting in poor flexibility of the PU chains. However, the further increase of carbon chain length of the chain extender leads to the increase of hard segment content (HS, see Table 1), and hence the decrease of the elongation.

### 3.3 Shape memory Properties of bio-based polyurethanes

Cyclic tensile testing was used to characterize the shape recovery properties of the bio-PU with different chain extenders. Figure 6 displays the cyclic tensile curves of these samples with a 200% constant strain, and their recovery rates of each cycle are summarized in Table 3. We can see that the recovery rates of all samples increase with cyclic number and almost keep constant after the second cycle, which had been reported by other researchers.<sup>37, 38</sup> This result is due to that weak physical cross-linking points such as hydrogen bond were destructed in the first cycle, resulting in a permanent deformation, and the PUs almost formed an ideal elastomeric network after the first two cycles.<sup>39, 40</sup> Therefore, the synthesized bio-PU exhibit a recovery rate higher than 90% after the following cycles.

Moreover, the recovery rate of the first cycle increases with the increase of the carbon chain length of the chain extender. This is because the bio-PU from the chain extender with the long carbon chain length has a lower  $T_g$ , leading to lower permanent deformation. For all synthesized bio-PU, their  $T_g$ s are higher than the testing temperature (25 °C), resulting in relatively high permanent deformation and low recovery rate of the first cycle. Compared with other bio-PU, the bio-PU-CHDM

exhibits better shape recovery properties. It has been reported that the increase of the micro-phase separation in PUs facilitates to improve the shape-memory properties.<sup>1,41</sup> Figure 7 shows the phase morphology of the obtained bio-based shape memory PUs from tapping mode AFM. Previous researchers had proved that soft segments correspond to darker regions and hard segments to bright regions in the phase images.<sup>42-44</sup> From the images of AFM, as the carbon chain length of the chain extender increases from bio-PU-EG to bio-PU-DDO, the micro-phase separation becomes more developed. This demonstrates that the bio-PU from the chain extender with long carbon chain length shows better shape-memory properties. Although the micro-phase separation of the bio-PU-CHDM is considerable with bio-PU-DDO, the higher shape recovery properties of the bio-PU-CHDM may originate from the asymmetrical non-planar ring structure of CHDM acting as “molecular spring”, which could absorb the external stress and stabilize the physical crosslinks.<sup>45</sup>

Furthermore, the shape memory properties of the synthesized bio-PUs at body temperature are also measured. Figure 8 exhibits the shape recovery process of bio-PU-CHDM at body temperature (37 °C). The sample was changed into a bending shape at 37 °C and then cooled rapidly to room temperature and it reached the original shape state in 1 min at 37 °C. Similarly, the recovery time of bio-PU-BDO is about 2 min. As the carbon chain length of the chain extender increases, the recovery time decreases. Moreover, the recovery rate of the broken samples ( $R_b$ ) was also used to characterize the shape memory properties, as listed in Table 3. The bio-PU-CHDM shows the highest shape recovery rate (92%). These results further indicate that the

non-planar ring structures in the hard segments have a positive effect on the shape memory.

#### 4. Conclusions

A series of bio-based shape memory PUs from polylactide copolymer diols and different chain extenders were successfully synthesized and characterized. The bio-based PUs have low Young's modulus (34.7 MPa) and high elongation (434.0%). As the carbon chain length of the chain extender increased from bio-PU-EG to bio-PU-DDO, the  $T_g$  values decreased and micro-phase separation became more developed, leading to the improvement of the shape-memory properties. The bio-PU with the non-planar ring structure of CHDM displays a highest shape recovery rate. All the synthesized bio-based PUs exhibit good shape memory behavior at the body temperature, which are promisingly applied in many medical devices.

#### Acknowledgements

The research is financially supported by the National Natural Science Foundation of China (Grant no. 21404112), Ningbo Key Scientific and Technological Project (Grant no. 2014B10023), Ningbo Natural Science Foundation (Grant no. 2015A610016), Ningbo Science and Technology Innovation Team (Grant no. 2015B11003), and Open Project of Key Laboratory of Marine Materials and Related Technologies (Grant no. 2016K07).

#### References

1. C. Liu, H. Qin and P. T. Mather, *Journal of Materials Chemistry*, 2007, **17**, 1543-1558.

2. A. Lendlein, *Journal of Materials Chemistry*, 2010, **20**, 3332-3334.
3. X. Qi, X. Yao, S. Deng, T. Zhou and Q. Fu, *Journal of Materials Chemistry A*, 2014, **2**, 2240-2249.
4. Q. Zhao, H. J. Qi and T. Xie, *Progress in Polymer Science*, 2015, **49-50**, 79-120.
5. C. M. Yakacki, R. Shandas, C. Lanning, B. Rech, A. Eckstein and K. Gall, *Biomaterials*, 2007, **28**, 2255-2263.
6. A. Lendlein and R. Langer, *Science*, 2002, **296**, 1673-1676.
7. L. Xue, S. Dai and Z. Li, *Journal of Materials Chemistry*, 2012, **22**, 7403-7411.
8. D. J. Maitland, M. F. Metzger, D. Schumann, A. Lee and T. S. Wilson, *Lasers in Surgery and Medicine*, 2002, **30**, 1-11.
9. W. Small, P. Singhal, T. S. Wilson and D. J. Maitland, *Journal of materials chemistry*, 2010, **20**, 3356-3366.
10. D. Rickert, A. Lendlein, I. Peters, M. A. Moses and R.-P. Franke, *European Archives of Oto-Rhino-Laryngology and Head & Neck*, 2006, **263**, 215-222.
11. E. Zini, M. Scandola, P. Dobrzynski, J. Kasperczyk and M. Bero, *Biomacromolecules*, 2007, **8**, 3661-3667.
12. J. N. Rodriguez, F. J. Clubb, T. S. Wilson, M. W. Miller, T. W. Fossum, J. Hartman, E. Tuzun, P. Singhal and D. J. Maitland, *Journal of Biomedical Materials Research Part A*, 2014, **102**, 1231-1242.
13. W. Small, M. F. Metzger, T. S. Wilson and D. J. Maitland, *Selected Topics in*

- Quantum Electronics, IEEE Journal of*, 2005, **11**, 892-901.
14. T. Takahashi, N. Hayashi and S. Hayashi, *Journal of Applied Polymer Science*, 1996, **60**, 1061-1069.
  15. L. Xue, S. Dai and Z. Li, *Macromolecules*, 2009, **42**, 964-972.
  16. S. Y. Gu and X. F. Gao, *RSC Advances*, 2015, **5**, 90209-90216.
  17. L. Zhang, M. Huang, R. Yu, J. Huang, X. Dong, R. Zhang and J. Zhu, *Journal of Materials Chemistry A*, 2014, **2**, 11490-11498.
  18. S. M. Hasan, J. E. Raymond, T. S. Wilson, B. K. Keller and D. J. Maitland, *Macromolecular Chemistry and Physics*, 2014, **215**, 2420-2429.
  19. P. Singhal, W. Small, E. Cosgriff-Hernandez, D. J. Maitland and T. S. Wilson, *Acta Biomaterialia*, 2014, **10**, 67-76.
  20. C. Zhang, S. A. Madbouly and M. R. Kessler, *Acs Applied Materials & Interfaces*, 2015, **7**, 1226-1233.
  21. L. Zhang, Y. Jiang, Z. Xiong, X. Liu, H. Na, R. Zhang and J. Zhu, *Journal of Materials Chemistry A*, 2013, **1**, 3263-3267.
  22. S. Miao, N. Callow, P. Wang, Y. Liu, Z. Su and S. Zhang, *J Am Oil Chem Soc*, 2013, **90**, 1415-1421.
  23. S. Miao, P. Wang, Z. Su, Y. Liu and S. Zhang, *European Journal of Lipid Science and Technology*, 2012, **114**, 1345-1351.
  24. E. del Rio, G. Lligadas, J. Carlos Ronda, M. Galia, V. Cadiz and M. A. R. Meier, *Macromolecular Chemistry and Physics*, 2011, **212**, 1392-1399.
  25. S. Thakur and N. Karak, *RSC Advances*, 2013, **3**, 9476-9482.

26. Y. Xu, Z. Petrovic, S. Das and G. L. Wilkes, *Polymer*, 2008, **49**, 4248-4258.
27. M. F. Sonnenschein, V. V. Ginzburg, K. S. Schiller and B. L. Wendt, *Polymer*, 2013, **54**, 1350-1360.
28. M. Xie, L. Wang, J. Ge, B. Guo and P. X. Ma, *Acs Applied Materials & Interfaces*, 2015, **7**, 6772-6781.
29. T. Tsujimoto and H. Uyama, *Acs Sustainable Chemistry & Engineering*, 2014, **2**, 2057-2062.
30. X. Zheng, S. Zhou, X. Li and J. Weng, *Biomaterials*, 2006, **27**, 4288-4295.
31. L. Peponi, I. Navarro-Baena, A. Sonseca, E. Gimenez, A. Marcos-Fernandez and J. M. Kenny, *European Polymer Journal*, 2013, **49**, 893-903.
32. W. S. Wang, P. Ping, X. S. Chen and X. B. Jing, *Polymer International*, 2007, **56**, 840-846.
33. W. S. Wang, P. Ping, X. S. Chen and X. B. Jing, *European Polymer Journal*, 2006, **42**, 1240-1249.
34. P. Singhal, J. N. Rodriguez, W. Small, S. Eagleston, J. Van de Water, D. J. Maitland and T. S. Wilson, *Journal of polymer science. Part B, Polymer physics*, 2012, **50**, 724-737.
35. X. Xiao, D. Kong, X. Qiu, W. Zhang, F. Zhang, L. Liu, Y. Liu, S. Zhang, Y. Hu and J. Leng, *Macromolecules*, 2015, **48**, 3582-3589.
36. H. C. Ki and O. Ok Park, *Polymer*, 2001, **42**, 1849-1861.
37. P. Ping, W. Wang, X. Chen and X. Jing, *Journal of Polymer Science Part B: Polymer Physics*, 2007, **45**, 557-570.



38. B. K. Kim, Y. J. Shin, S. M. Cho and H. M. Jeong, *Journal of Polymer Science Part B: Polymer Physics*, 2000, **38**, 2652-2657.
39. A. Lendlein and S. Kelch, *Angewandte Chemie International Edition*, 2002, **41**, 2034-2057.
40. Z. Yong, H. Jinlian, Y. Lap-Yan, L. Yan, J. Fenglong and Y. Kwok-wing, *Smart Materials and Structures*, 2006, **15**, 1385.
41. S. Chen, Q. Cao, B. Jing, Y. Cai, P. Liu and J. Hu, *Journal of Applied Polymer Science*, 2006, **102**, 5224-5231.
42. C. Li, J. Liu, J. Li, F. Shen, Q. Huang and H. Xu, *Polymer*, 2012, **53**, 5423-5435.
43. A. Aneja and G. L. Wilkes, *Polymer*, 2003, **44**, 7221-7228.
44. P. Schön, K. Bagdi, K. Molnár, P. Markus, B. Pukánszky and G. Julius Vancso, *European Polymer Journal*, 2011, **47**, 692-698.
45. L. Zhang, S. S. Shams, Y. Wei, X. Liu, S. Ma, R. Zhang and J. Zhu, *Journal of Materials Chemistry A*, 2014, **2**, 20010-20016.

## Figure legends

**Scheme 1** Synthetic route for bio-SMPUs.

**Figure 1** FTIR spectra of the obtained bio-PU.

**Figure 2**  $^1\text{H}$  NMR spectra of the obtained bio-PU.

**Figure 3** DSC curves of the obtained bio-PU.

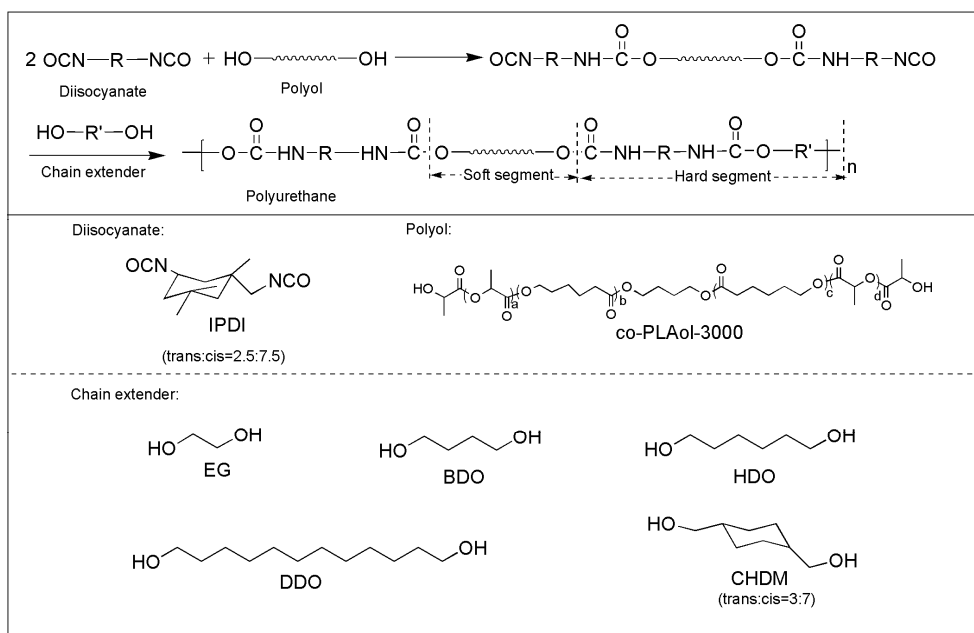
**Figure 4** TGA curves of the obtained bio-PU.

**Figure 5** Stress-strain curves of the obtained bio-PU.

**Figure 6** Cyclic tensile curves of the bio-SMPUs.

**Figure 7** AFM height and phase images of the bio-SMPUs: (a) bio-PU-EG; (b) bio-PU-BDO; (c) bio-PU-HDO; (d) bio-PU-DDO; (e) bio-PU-CHDM.

**Figure 8** Recovery process of shape memory bio-PU-CHDM at 37 °C.



**Scheme 1** Synthetic route for bio-SMPUs.

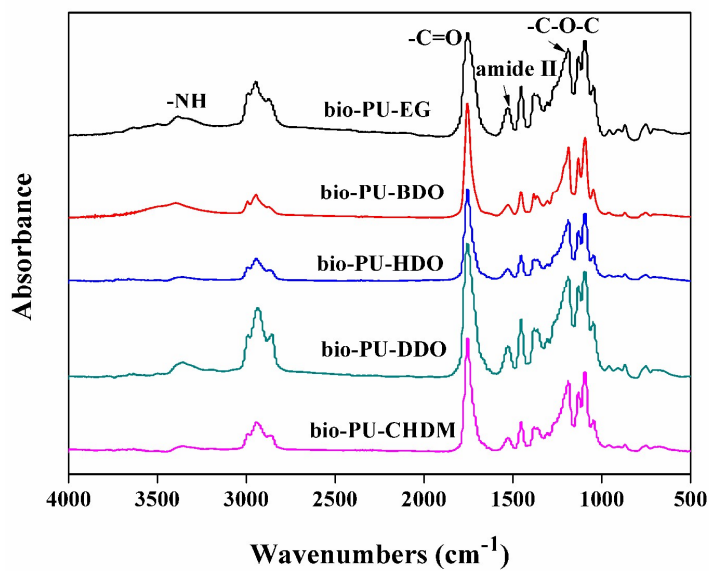


**Figure 1** FTIR spectra of the obtained bio-PU.

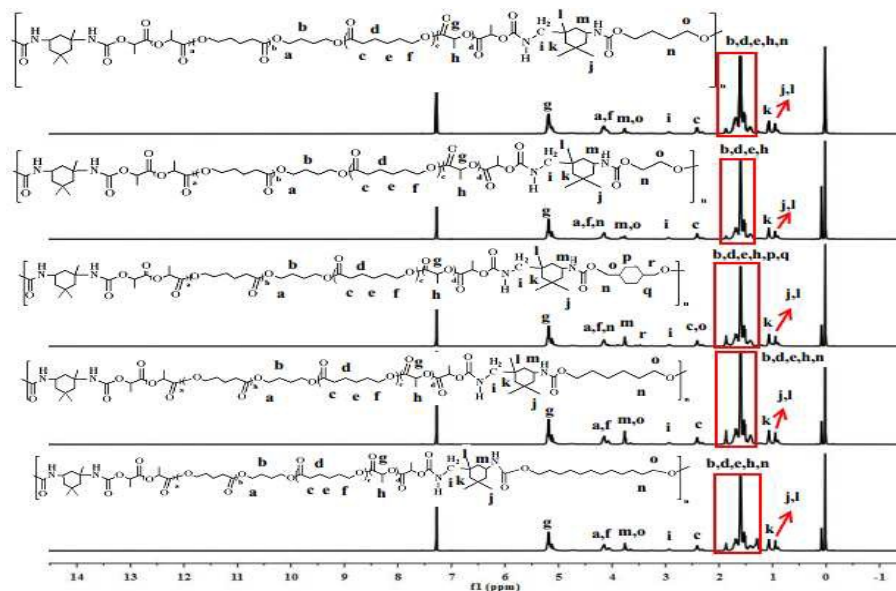


Figure 2  $^1\text{H}$  NMR spectra of the obtained bio-PU.

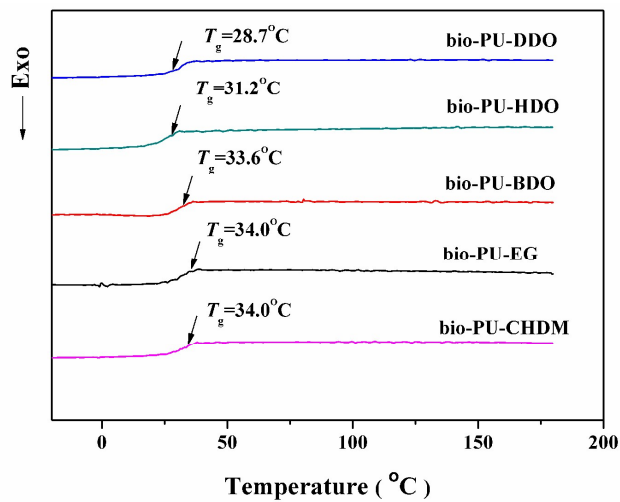


Figure 3 DSC curves of the obtained bio-PU.

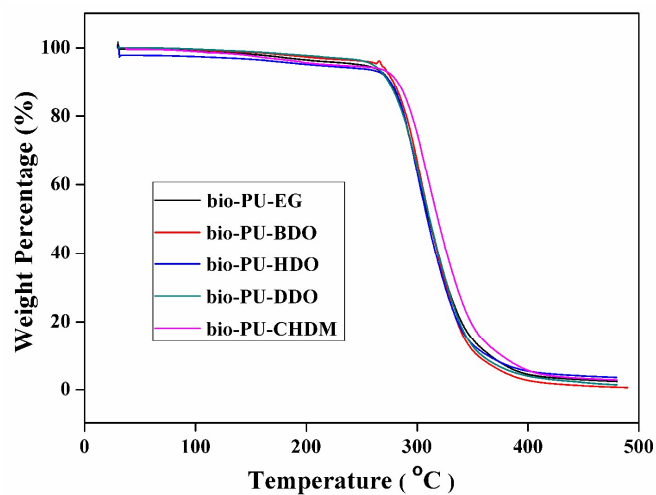


Figure 4 TGA curves of the obtained bio-PU.

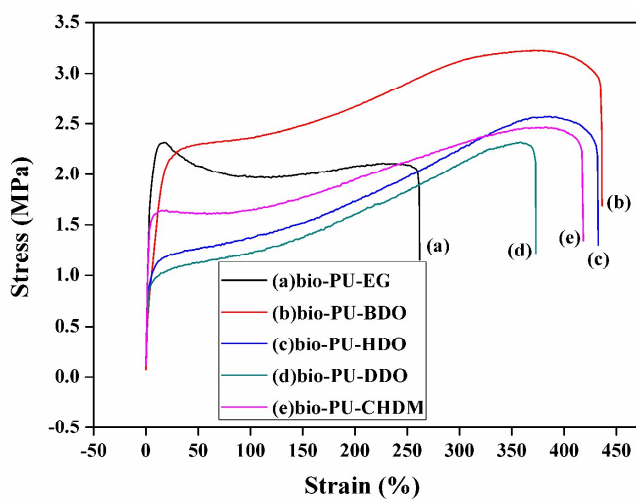
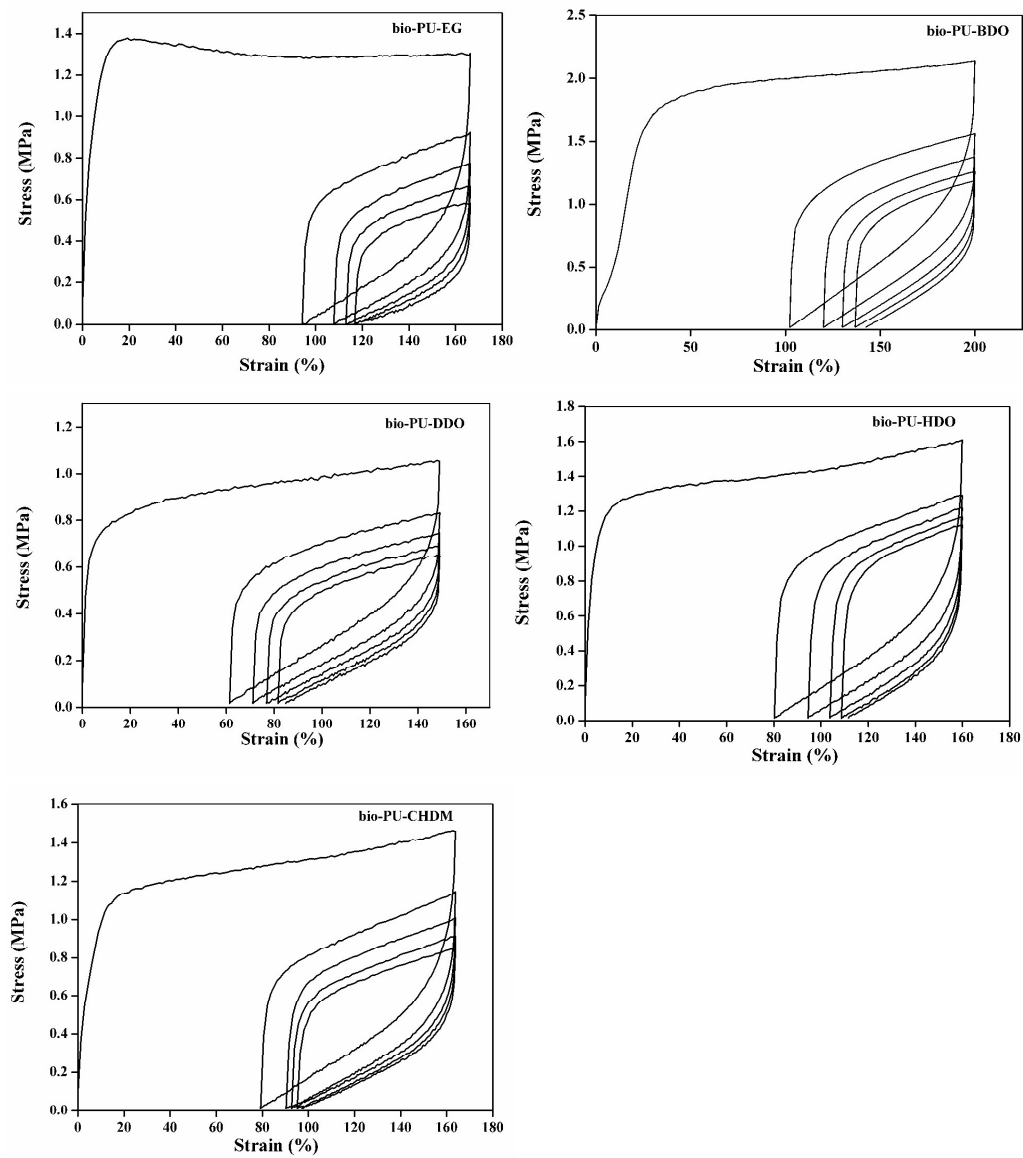
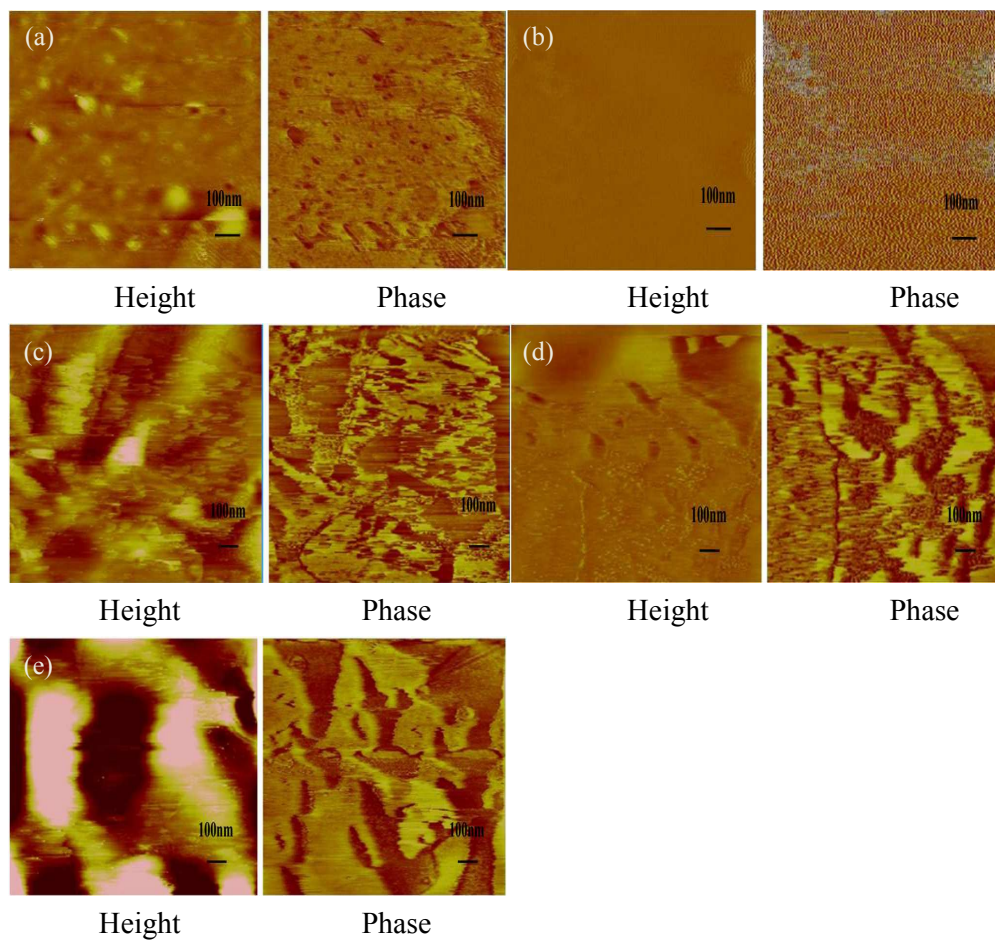


Figure 5 Stress-strain curves of the obtained bio-PU.



**Figure 6** Cyclic tensile curves of the bio-SMPUs.



**Figure 7** AFM height and phase images of the bio-SMPUs: (a) bio-PU-EG; (b) bio-PU-BDO; (c) bio-PU-HDO; (d) bio-PU-DDO; (e) bio-PU-CHDM.

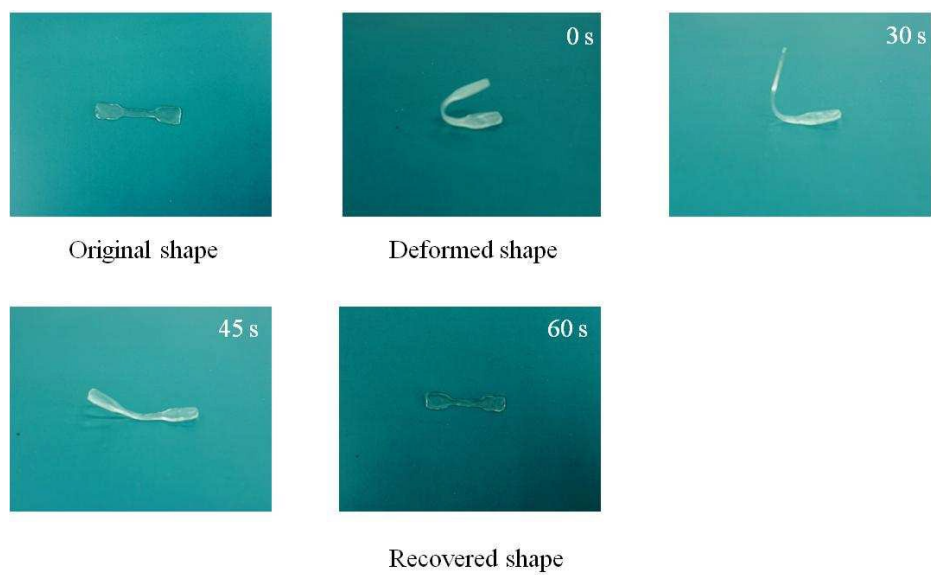


**Figure 8** Recovery process of shape memory bio-PU-CHDM at 37 °C.



**Table 1** The detail information of the obtained bio-PU

	Chain extenders	HS (wt%) <sup>a</sup>	$M_w$ <sup>b</sup>	$M_w/M_n$ <sup>b</sup>
bio-PU-EG	EG	14.4	$1.8 \times 10^4$	2.0
bio-PU-BDO	BDO	15.1	$2.1 \times 10^4$	2.1
bio-PU-HDO	HDO	15.7	$2.7 \times 10^4$	2.1
bio-PU-DDO	DDO	17.7	$2.7 \times 10^4$	2.1
bio-PU-CHDM	CHDM	16.4	$2.6 \times 10^4$	2.1

<sup>a</sup> The hard segment weight percent (HS, wt%), which is defined as the percent by weight of the chain extender and IPDI in the polyurethane. <sup>b</sup> Measured by GPC.

**Table 2** Thermal and mechanical properties of the bio-PU

	$T_g$ (°C)	$T_{5\%}$ (°C) <sup>a</sup>	$T_{max}$ (°C) <sup>b</sup>	Tensile Strength (MPa)	Elongation (%)	Young's modulus (MPa)
bio-PU-EG	34.0	251.0	300.6	$2.3 \pm 0.1$	$261.3 \pm 15$	$59.4 \pm 2.3$
bio-PU-BDO	33.6	267.8	304.1	$3.2 \pm 0.2$	$434.0 \pm 25$	$34.7 \pm 1.7$
bio-PU-HDO	31.2	208.0	300.7	$2.6 \pm 0.1$	$432.0 \pm 25$	$35.1 \pm 1.8$
bio-PU-DDO	28.7	260.6	300.6	$2.3 \pm 0.1$	$372.6 \pm 18$	$36.0 \pm 2.0$
bio-PU-CHDM	34.0	255.6	306.3	$2.4 \pm 0.1$	$417.0 \pm 20$	$58.6 \pm 2.1$

<sup>a</sup>  $T_{5\%}$  is the 5% weight-loss temperature of the samples. <sup>b</sup>  $T_{max}$  is the temperature of the maximum rate of weight-loss of the samples.

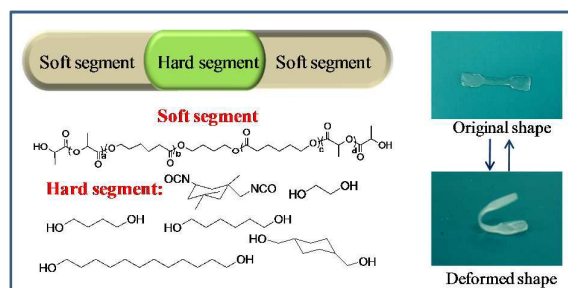
**Table 3** The recovery rate at 200% strain of the cyclic tensile tests.

	$R_r(1)$ (%)	$R_r(2)$ (%)	$R_r(3)$ (%)	$R_r(4)$ (%)	$R_r(5)$ (%)	$R_b$ (%) <sup>a</sup>
bio-PU-EG	$43 \pm 0.2$	$81 \pm 0.3$	$91 \pm 0.1$	$93 \pm 0.2$	$94 \pm 0.5$	$88 \pm 0.3$
bio-PU-BDO	$49 \pm 0.1$	$82 \pm 0.2$	$87 \pm 0.3$	$90 \pm 0.1$	$91 \pm 0.2$	$88 \pm 0.1$
bio-PU-HDO	$50 \pm 0.3$	$82 \pm 0.4$	$86 \pm 0.1$	$91 \pm 0.2$	$94 \pm 0.5$	$90 \pm 0.4$
bio-PU-DDO	$51 \pm 0.2$	$85 \pm 0.5$	$93 \pm 0.4$	$93 \pm 0.4$	$95 \pm 0.8$	$90 \pm 0.2$
bio-PU-CHDM	$52 \pm 0.3$	$87 \pm 0.1$	$97 \pm 0.1$	$96 \pm 0.1$	$97 \pm 0.6$	$92 \pm 0.1$

<sup>a</sup>  $R_b$  is the recovery rate of the samples measured in the next 15s after the break during tensile tests.

## Bio-based Polyurethanes with Shape Memory Behavior at Body Temperature: Effect of Different Chain Extenders

Lin Gu<sup>1\*</sup>, Bin Cui<sup>1,3</sup>, Qing-Yun Wu<sup>2</sup>, Haibin Yu<sup>1\*</sup>



The chain extenders are used to adjust the transition temperatures and shape memory properties of bio-based shape memory polyurethanes.

\* Corresponding author: Tel.: +86 0574 87911126.

E-mail addresses: gulin1985@gmail.com; haibinyu@nimte.ac.cn